Cell Motility and the Cytoskeleton 43:296–309 (1999)

Analysis of Actin Filament Bundle Dynamics During Contact Formation in Live Epithelial Cells

Mira F. Krendel and Edward M. Bonder*

Program in Cellular and Molecular Biodynamics, Department of Biological Sciences, Rutgers University–Newark, Boyden Hall, Newark, New Jersey

The actin cytoskeleton is an integral component of the cell-cell adherens junction complex. We used fluorescence labeling of actin filaments and time-lapse laser scanning confocal microscopy to investigate the functional relationship between the organization of the actin cytoskeleton and formation of adherens junctions in live epithelial cells. Rhodamine-phalloidin was loaded into cultured cells by wounding epithelial monolayers in the presence of fluorescent analog. Rhodamine-phalloidin was incorporated into the actin filaments in stress fibers, circumferential bundles, and marginal bundles. Cells containing labeled actin filaments appeared physiologically normal since the rates of migration, rates of pseudopodial protrusion/retraction, ability to form contacts, and sensitivity to cytochalasin B were equivalent to non-loaded, control epithelial cells. Marginal actin bundles initially formed as bow-shaped bundles that were observed to straighten as the bundles flowed rearward and away from the free cell edge. When lamellae from adjacent cells made contact, rearward flow of marginal bundles ceased and the bundles started to disassemble with higher frequency. Next, we observed the formation of arc-like bundles at the edges of contacting cells, a position suggestive of a role in lateral expansion of the contact. During later stages of contact formation, new actin bundles assembled along the length of the expanding cell-cell boundary. These newly formed bundles are likely to participate in the establishment of the initial cadherin/actin cytoskeleton linkage and eventually form the circumferential bundles at the cell-cell adherens junction. Additionally, indirect immunolocalization studies characterized the location of myosin-II. A model is presented describing the function of the spatial and temporal dynamics of actin filament bundles and myosin-II activity in the formation of adherens junctions. Cell Motil. Cytoskeleton 43:296–309, 1999.

Key words: actin cytoskeleton; adherens junctions; myosin; confocal microscopy

INTRODUCTION

Cell-cell contacts are fundamentally important to all multicellular organisms since they serve to establish a means for tissue development, communication, and physical integrity. Adherens junctions are highly ubiquitous cell-cell contacts found in virtually all solid tissues where they form the structural basis of cell-cell adhesion [Gumbiner, 1996]. Principal components of adherens junctions are cadherins, actin filaments, and cytoplasmic protein plaques linking cadherins to the actin cytoskeleton. Cadherins are a superfamily of cell and tissue specific single-pass transmembrane proteins, which interact with β-, γ-, and α-catenins at cytoplasmic adhesion plaques. α-catenin anchors the cadherin-catenin complex to actin filaments, either directly or through interaction with vinculin and/or α-actinin [Geiger et al., 1995].

Contract grant sponsor: Charles and Johanna Busch Memorial Fund.

*Correspondence to: Edward M. Bonder, Department of Biological Sciences, Rutgers University–Newark, University Heights, 101 Warren Street, Newark, NJ 07102. E-mail: ebonder@andromeda.rutgers.edu

Received 14 January 1999; accepted 30 April 1999

During contact formation in epithelial cells, E-cadherin and α- and β-catenins become strongly associated with the actin cytoskeleton as indicated by their resistance to detergent extraction [Adams et al., 1996]. Disruption of the actin cytoskeleton [Angres et al., 1996] or elimination of the interaction between cadherins and actin filaments through loss of catenin function [Ozawa et al., 1990] prevents establishment of intercellular adhesion. Furthermore, the small G-proteins rho and rac, which are involved in regulation of actin organization, are also required for normal assembly of intercellular adherens junctions [Braga et al., 1997]. Consequently, functional cadherin-based adherens junctions are proposed to rely upon appropriate temporal and spatial organization of the actin cytoskeleton during junctional complex formation. While the importance of an association between the actin cytoskeleton and adherens junctions is well established, there is, unfortunately, a modicum of information available about the dynamic activity of the actin cytoskeleton during assembly of these junctions [Adams and Nelson, 1998]. The absence of such knowledge makes it difficult to propose a mechanistic framework for the role of the actin cytoskeleton in facilitating assembly of adherens junctions.

In a prior study, we used time-lapse video-DIC microscopy, laser optical tweezers, and fluorescence microscopy of fixed cells to initially characterize the relationship between formation of cadherin-containing junctions and the actin cytoskeleton [Gloushankova et al., 1997]. It was found that contact formation modified both cortical flow of membrane glycoproteins and the overall organization of the actin cytoskeleton [Gloushankova et al., 1997]. Based on those observations, a hypothetical model was presented whereby rapid structural reorganization of the actin cytoskeleton in contacting lamellae leads to changes in the orientation of myosin-driven tension, resulting in expansion of the intercellular contact.

In the present report, we employed fluorescence cytochemistry and laser scanning confocal microscopy of live epithelial cells to image the in vivo dynamics of the actin cytoskeleton within lamellae during initiation and formation of adherens junctions. Actin filaments were labeled with trace amounts of fluorescent phalloidin by wound-loading monolayers of epithelial cells. Cells with fluorescent phalloidin-labeled actin filaments were structurally and functionally indistinguishable from control, non-labeled cells. We determined that marginal bundles, located at free cell edges, exhibited a previously unrecognized form of retrograde flow, which may be linked to myosin-II activity. Upon cell-cell contact, there was breakage and disassembly of existing bundles, formation of new actin bundles at the cell-cell border, and assembly and lateral movement of arc-like actin bundles at the edges of the cell-cell contacts. Contraction of disassembling marginal bundles together with the presence of myosin-II in actin arcs provided evidence supporting an essential role for myosin-dependent tension during formation of intercellular junctions. The findings presented in this report provide new mechanistic insight into how the spatial and temporal dynamic activity of the actin cytoskeleton facilitates adherens junction assembly and maturation.

MATERIALS AND METHODS

Cell Culture and Immunofluorescence Microscopy

IAR-2 rat hepatocytes were plated on coverslips and grown to confluency in DMEM supplemented with 10% fetal calf serum. Narrow wounds were created by gently scraping the slide with a sterile syringe needle and observations were made after 3–4 hours of incubation, at which time the wound started to close [Gloushankova et al., 1997]. Indirect immunofluorescence localization of β-catenin and myosin-II and rhodamine-phalloidin labeling of actin filaments in fixed cells were carried out as previously described [Gloushankova et al., 1998].

Wound Loading of Rhodamine-Phalloidin

Rhodamine-phalloidin was freshly prepared by taking a 6.6 μM stock solution in methanol, drying it to remove methanol, and then redissolving the rhodamine-phalloidin in PBS to final concentrations ranging from 13.2 to 66 μM. Coverslips with attached cell monolayers were removed from their culture dishes, placed into fresh, sterile dishes, and 5 μl of rhodamine-phalloidin were immediately pipetted onto the residual thin film of medium (measured volume of film was 15–20 μl) covering the cells. Monolayers were wounded using a sterile syringe needle, rinsed with warm DMEM, and incubated for 3–4 hours in DMEM with fetal calf serum prior to observation.

Fluorescence Observations of IAR-2 Cells

Coverslips, with cells recovering from injury, were mounted into sealed observation chambers and fluorescent actin filaments were imaged using a Bio-Rad MRC-1024 Laser Scanning Confocal Microscope System (Hercules, CA) equipped with Nikon (Melville, NY) optics. Neutral density filters were used to set power of the excitation laser to either 3 or 10% of its maximum output and images were collected at 1-min intervals by averaging 3–5 frames taken in slow scan mode. By this imaging protocol, it was possible to observe the activity of bundles of actin filaments within cells for approximately 30 min without significant loss of signal due to photobleaching. Actin meshworks in lamellipodia could also be imaged using these methods; however, the cells needed to be wounded in the presence of the highest concentration of

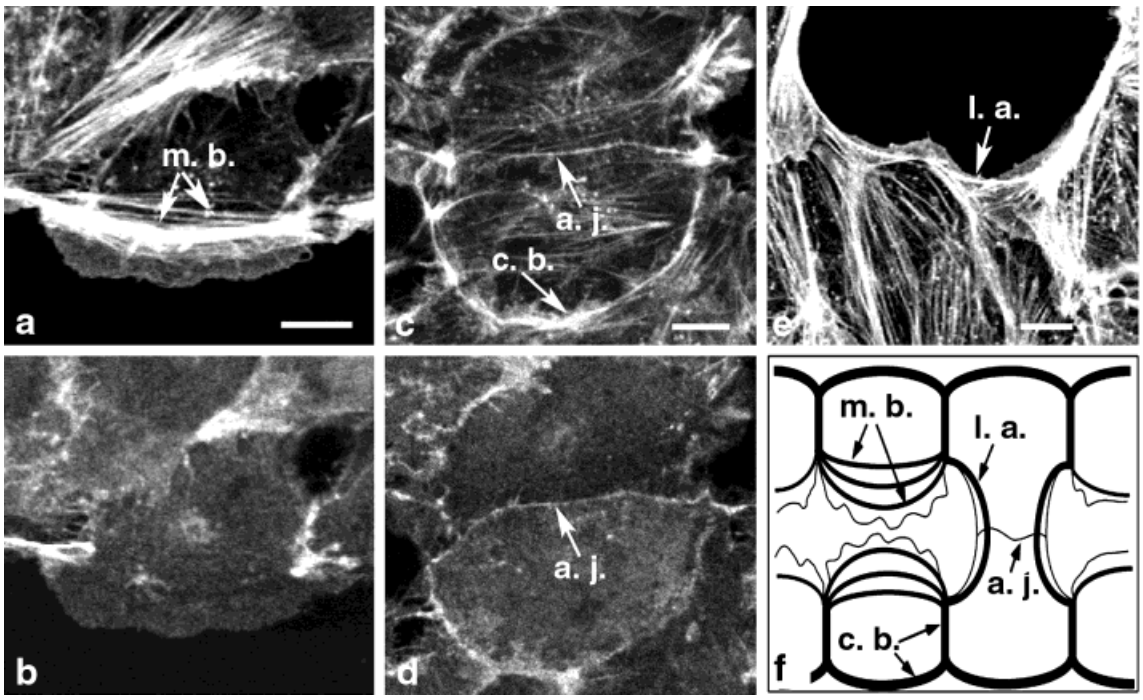

Fig. 1. Organization of the actin cytoskeleton and the associated cell adhesion protein, β-catenin, in IAR-2 cells. **a–e:** Cells were fixed and labeled with rhodamine-phalloidin (a,c,e) and monoclonal anti-β-catenin antibodies (b,d). Cells located at the free edge of the wound contained prominent marginal actin bundles (see a, m.b. = marginal bundle) that were not associated with β-catenin. During contact formation, thin actin bundles that colocalized with β-catenin formed along the adherens junctions (c and d; a.j. = adherens junctions). Actin bundles associated with newly formed adherens junctions were similar in appearance and β-catenin enrichment to circumferential actin belts observed in mature cell-cell contacts (c; c.b. = circumferential bundle). Expanding contacts also contained prominent lateral actin arcs (e; l.a. = lateral arc). Bar = 10 μm. **f:** Schematic summary of the actin organization in IAR-2 cells prior to and during contact formation. Free cell edges prior to contact formation contain marginal bundles (m.b.). Newly formed contacts contain adherens junction-associated actin bundles (a.j.) and lateral arcs (l.a.) while mature cell-cell contacts are supported by circumferential actin bundles (c.b.).

rhodamine-phalloidin (66 μM) and imaged using confocal laser setting at 30–100% maximal intensity. Unfortunately, a single imaging mode capable of appropriately monitoring both marginal bundles and actin meshworks was not possible due to the large disparity in fluorescence intensity between bundles and meshworks.

Image analysis and measurements of the velocity of actin bundle movement were performed over 5–10-min periods using MetaMorph image processing software (Universal Imaging Corporation, West Chester, PA). To determine the frequency of marginal bundle snapping, 10–30-min-long time-lapse confocal sequences of individual non-contacting and contacting cells were analyzed and the average number of bundles snapping per 10 min was calculated. Time-lapse videos of protrusion and retraction of the leading edges of cells were made by first locating loaded cells using epifluorescence microscopy and then recording DIC images of the loaded cells onto S-VHS videotape. Quantitation of cell edge activity was carried out as previously described [Gloushankova et al., 1995]. The average number of bundles snapping per 10 min before vs. after contact and the average velocity of forward movement of leading edges of labeled and non-labeled cells were compared by Student's *t*-test.

RESULTS

Summary of Actin Cytoskeleton and β-Catenin Organization During Formation of Cell-Cell Contacts

Cells at the edge of a wound possessed four distinct types of actin filament structures: meshworks of filaments in the lamellipodia; stress fibers in the cell body; marginal bundles of filaments running along the edge of the lamella-cell body boundary; and circumferential bundles associated with adherens junctions (Fig. 1). Marginal bundles were located at free, non-contacting lamellar edges where they usually consisted of multiple thin bundles oriented parallel to the free edge (Fig. 1a,f). Marginal bundles were not associated with β-catenin except at their ends where an adherens junction formed with the adjacent cell (Fig. 1b). Stress fibers were straight and without apparent preferential orientation relative to the edge of the cell. Both marginal actin bundles and

stress fibers were located in the basal portion of the cells, near the substrate. Regions of cells in contact with neighboring cells possessed prominent circumferential bundles of actin filaments that lined the perimeter of the apical portion of the cell (Fig. 1c,f) and were co-localized with β-catenin (Fig. 1c,d). As contacts matured, a thin bundle of actin filaments associated with β-catenin appeared along the length of the cell-cell contact (Fig. 1c,d). During formation and spreading of cell-cell contacts, adjacent cells formed prominent arcs of actin filaments at the lateral edges of the contact where they have been proposed to participate in contact expansion (Fig. 1) [Gloushankova et al., 1997].

Wound Loading of Rhodamine-Phalloidin Into Live Cells

The fluorescent probe rhodamine-phalloidin has been successfully microinjected into tissue culture cells, without detectable deleterious effects, to examine actin filament dynamics in live cells [Wang, 1987; Wehland and Weber, 1981]. Employing the basic wounding strategy Brock et al. [1996] used to load sheets of epithelial cells with inhibitors of small G proteins, we loaded rhodamine-phalloidin into epithelial cells during the process of generating scrape wounds in cultured monolayers of cells. Wound loading provided an efficient method to simultaneously introduce rhodamine-phalloidin into multiple cells lying along the edge of the wound without needing to microinject the fluorescent probe into cells that may already have been traumatized during wounding. Observations of live cells showed concentrated rhodamine-phalloidin labeling of actin filaments within marginal bundles, stress fibers, and circumferential bundles, as early as 30 min after wounding with an average of 30–60% of the cells at the wound edge getting labeled. Combining the highest dosage of rhodamine-phalloidin with laser scanning confocal imaging at high laser intensities made it possible to detect labeling of actin filaments within lamellipodia at the leading edge of cells. For the present report, we were concerned with the dynamic activities of the bundles of actin filaments, primarily the marginal bundle; therefore, low rhodamine-phalloidin concentrations and low laser intensities were used in the reported experiments. Based on the work of Brock et al. [1996], we estimate that when cells were wounded in the presence of 13.3 μM rhodamine-phalloidin, ~0.13 μM label was loaded into the cells. This estimate is an order of magnitude lower in concentration than previously used to examine actin filament dynamics in live cells [Cao and Wang, 1990; Wang, 1987].

Cells loaded with rhodamine-phalloidin did not demonstrate any detectable change either in general morphology or actin filament organization as compared to non-loaded cells. Observations using DIC-microscopy showed that rhodamine-phalloidin–loaded cells were not rounded up or detached from the substrate. A comparison of two sets of wounds made on the same coverslip, one in the presence of PBS containing rhodamine-phalloidin and the other solely in PBS, detected no qualitative difference in the rates of wound closure. Quantitative comparisons by unpaired Student's *t*-test of the rates of leading edge advancement during wound healing between different sets of coverslips indicated no statistically significant difference between the rates in scrape-loaded (0.29 ± 0.075 μm/minute; mean ± SEM, $n = 10$) and control cells (0.34 ± 0.070 μm/minute; mean ± SEM, $n = 14$). A similar conclusion was drawn for a comparison between the rates of pseudopodial protrusion and retraction (not shown). Further, since binding of phalloidin to actin filaments can stabilize actin against depolymerization [Cooper, 1987], rhodamine-phalloidin–labeled cells were examined for sensitivity to depolymerization by cytochalasin B [Wang, 1987; Wehland and Weber, 1981]. There was no detectable protective effect in cells loaded with rhodamine-phalloidin since actin filaments organization and assembly was equally disrupted in labeled and unlabeled cells (data not shown). Consequently, wound loading cultured epithelial cells with fluorescent phalloidin appears to provide an appropriate experimental model to observe the activity of actin filament bundles in live cells.

Actin Filament Organization and Dynamics at the Free Cell Edge

Time-lapse laser scanning confocal microscopy of fluorescently labeled cells detected centripetal movement of marginal actin bundles, within lamellae, away from the cell edge and in a plane above the stress fibers that attached the cell to the substrate (Fig. 2). Marginal bundles formed at the base of the diffusely labeled actin meshworks present at the distal edge of the cell. Initially, the bundles had a curved shape that followed the general contour of the free edge of the cell (Fig. 2). The center of marginal bundles moved, relative to the substrate, at an average rate of 0.28 ± 0.006 μm/minute ($n = 23$ bundles in 7 cells). There was no observed correlation between the rate of rearward movement of marginal bundles and the rate of forward movement of the leading edge of the same cell (Table I; also see Fig. 2). A consequence of this movement and loss of curvature was that the overall length of marginal bundles decreased during their rearward excursion.

As individual marginal bundles moved away from the edge of the cell, we observed the formation of new bundles within the area of diffuse fluorescence at the leading edge. Similar to pre-existing marginal bundles, new bundles were curved and formed parallel to the

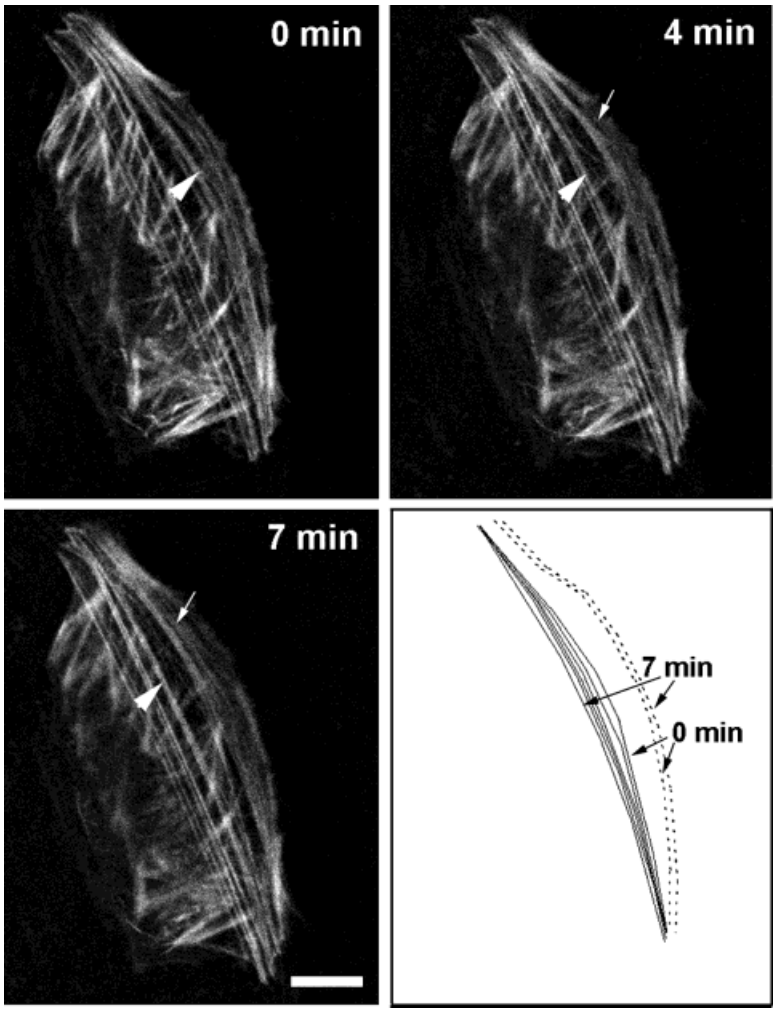

Fig. 2. Assembly and rearward flow of marginal actin bundles. The montage shows representative frames from a time-lapse sequence of images of an IAR-2 cell located at the free wound edge that was wound-loaded with rhodamine-phalloidin and observed over a 7-min period. During the period of observation, marginal actin bundles assembled at the leading edge of the cell (*arrow*). Marginal actin bundles located near the leading edge often underwent retrograde translocation (*arrowhead*); position of the bundle marked with the arrowhead during the 7-min interval is schematically represented (*solid lines*) along with the outline of the leading edge (*dashed lines*). Note that while the bundle was undergoing rearward flow, the leading edge of the cell was moving forward. Bar = 10 μm.

TABLE I. Comparison of the Rate of Rearward Actin Bundle Flow With the Velocity of Leading Edge Advance

Velocity of forward movement of the leading edge of a cell (μm/min)	Average velocity of rearward flow of actin bundles in the same cell relative to the substrate (μm/min) ± S.E.M. (n = number of bundles examined)
0	0.41 ± 0.045 (n = 4)
0.29	0.19 ± 0.014 (n = 4)
0	0.13 ± 0.014 (n = 2)
0.45	0.36 ± 0.033 (n = 3)
0	0.25 ± 0.010 (n = 4)
0	0.16 ± 0.013 (n = 3)
0.43	0.44 ± 0.027 (n = 3)

leading edge (Fig. 2). Consequently, there was continuous assembly of new bundles as previously assembled bundles moved centripetally. Stress fibers located in the cell body either remained stationary or moved forward together with the cell body. We did not observe de novo assembly of internal bundles. Instead, on a few occasions the innermost marginal bundles were observed to straighten and shorten while continuing their centripetal movement until they became similar in appearance and location to pre-existing internal bundles.

Occasionally, during centripetal movement, an individual bundle would develop a small non-fluorescent gap along its length, giving the impression of breakage within the bundle (Fig. 3). The remaining two segments of the bundle would shorten toward their ends at the lateral edges of the cell resulting in an increase in the size of the

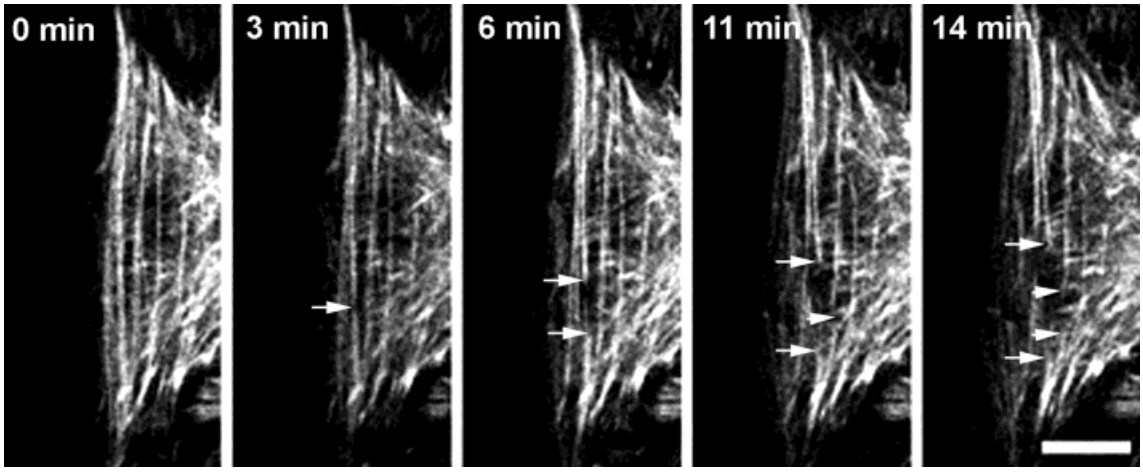

Fig. 3. Disassembly (''snapping'') of marginal actin bundles. An IAR-2 cell at the free wound edge was loaded with rhodamine-phalloidin and observed for 14 min. During this period, several marginal actin bundles were observed to rapidly disassemble (''snapping''). Disassembly started with formation of small non-fluorescent gaps (*arrow* at 3 min and *arrowhead* at 11 min). The gaps then proceeded to rapidly expand (*arrows* at 6, 11, and 14 min, and *arrowheads* at 14 min), leading, in some cases, to almost complete disassembly of the bundle fragments (see, for example, the short bottom fragment indicated with an arrow at 6, 11, and 14 min). Bar = 10 μm.

non-fluorescent gap in the middle of the bundle. During shortening, the remaining segments of the bundle appeared to increase in fluorescence intensity and thickness (Fig. 3, compare 3- and 6-min images), suggesting that the bundles were contracting. We termed this rapid shortening ''snapping'' since it was similar in appearance to the snapping back of a stretched rubber band after it is cut. The frequency of snapping at free cell edges was 0.4 observed events/10 min in 6 cells examined. We observed no identifiable correlation between the timing of snapping and the length of observation by the laser scanning confocal microscope, indicating that snapping was not due to a photo-toxic effect from laser illumination during data collection.

Actin Filament Dynamics During Cell-Cell Contact Formation

Formation of cell-cell adherens junctions leads to dramatic inhibition of functional activity of contacting lamellae as well as an accompanying change in the organization of the actin cytoskeleton [Gloushankova et al., 1997; Yap et al., 1997]. In situ observations of fluorescently labeled actin filament bundles provide an understanding of the mechanistic basis of these earlier reports. Upon formation of a stable cell-cell contact, there was a slowing or loss of rearward movement of marginal bundles of actin filaments (Figs. 4 and 5). With the slowed or stopped centripetal flow, there was temporary cessation of bundle formation in the area undergoing contact formation. At the same time, pre-existing marginal bundles exhibited a statistically significant increase in the frequency of snapping (1 observed event/10-min period, 12 cells analyzed) as compared to marginal bundles in non-contacting lamellae. In several instances, multiple cuts occurred along the length of individual bundles (Figs. 4 and 5).

As the marginal bundles stopped undergoing centripetal flow and started to disassemble, the expanding edges of the cell-cell contact exhibited an increase in the levels of fluorescently labeled actin. At these sites, bundles of actin filaments started to form arcs that lined the expanding boundary of the cell-cell contact. In some instances, the lateral arcs seemed to have formed from the ''frayed ends'' of marginal bundles that had snapped during earlier stages of contact formation (Figs. 4–6). The arcs continued moving laterally together with the expanding edge of the contact, giving the impression that the lateral arc was driving contact expansion (Fig. 6).

Additionally, as the contact expanded, new thin bundles of actin filaments started to assemble along the boundary of the two cells making contact (Figs. 4 and 5). The newly formed bundles did not undergo centripetal translocation but remained aligned along the cell-cell boundary and their elongation coincided with the expansion of the contact. Based on their appearance and location, the thin actin bundles along the axis of contact may serve as the structural basis for the formation of β-catenin-associated actin filament bundles seen in mature contacts (compare Fig. 1c,d with Figs. 4 and 5).

Localization of Myosin-II During Formation of Cell-Cell Contacts

A number of the dynamic properties of actin filament bundles observed in epithelial cells during cell-cell contact

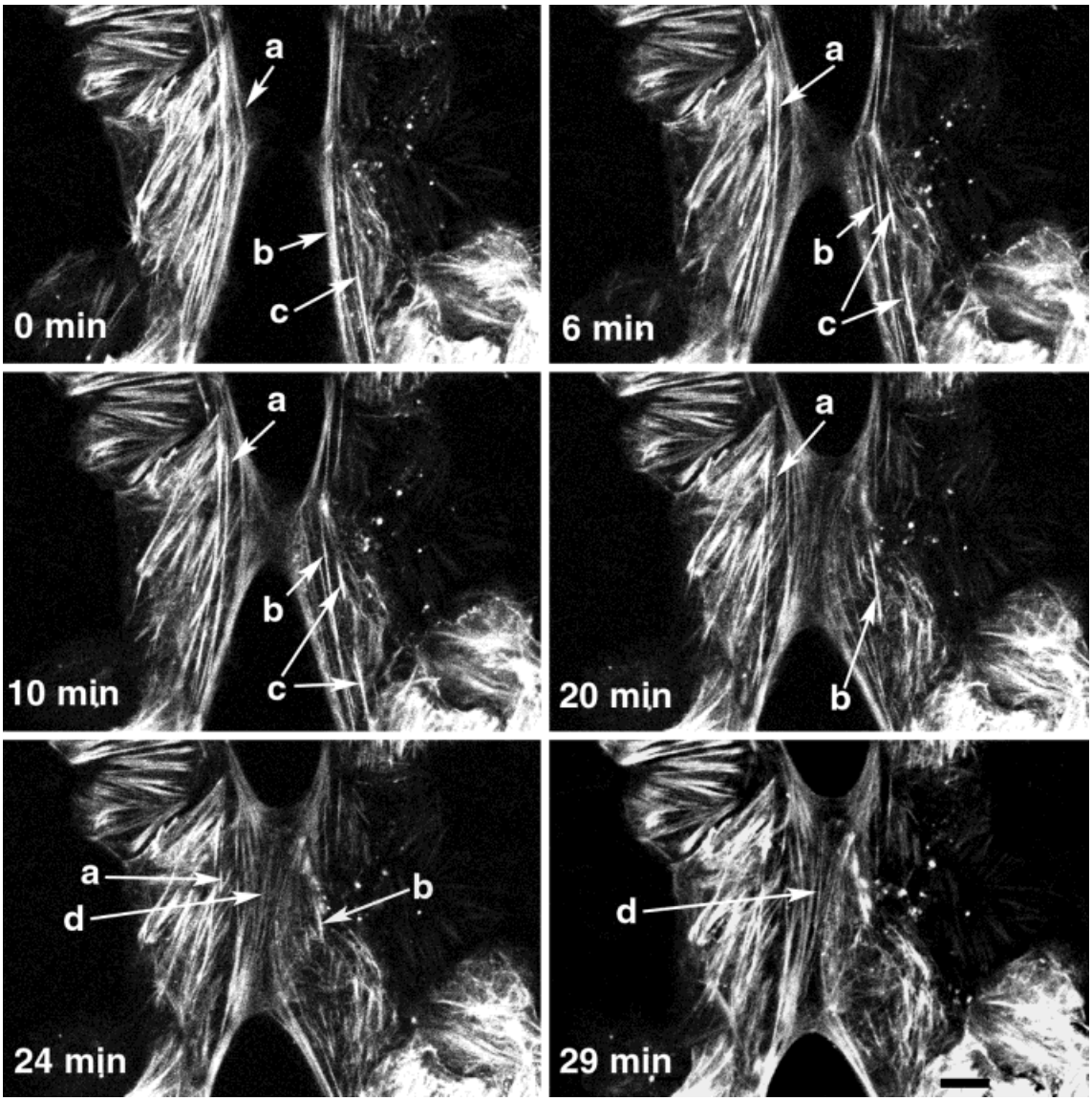

Fig. 4. Time-lapse observation of the reorganization of the actin cytoskeleton during contact formation. IAR-2 cells were loaded with rhodamine-phalloidin and observed during the process of cell-cell contact formation. Time indicated is relative to the first frame shown. Prior to contact formation marginal bundles **a, b,** and **c** were undergoing retrograde flow away from the cell edge. After formation of an initial contact (6 min), rearward actin flow stopped and marginal bundles underwent snapping. Notice breakage and shortening of bundles a, b, and c in frames corresponding to 6, 10, and 20 min after the beginning of the time-lapse sequence. By 24 min, bundle c completely disappeared and only short fragments of bundles a and b were left. As the contact expanded, new actin bundles were assembled along the cell-cell boundary (d). Bar = 10 μm.

could rely on contractile activity that is typically linked to myosin-II function. Furthermore, since myosin-II has been implicated in the process of healing small puncture wounds in epithelial sheets [Bement et al., 1993], the spatial distribution of myosin-II during cell-cell contact formation and subsequent spreading of the contact was determined. Anti-myosin-II antibody staining was observed along virtually all actin filament bundles, including marginal bundles, stress fibers, circumferential bundles, and lateral arcs. The staining pattern was periodic, resulting in a punctate appearance that is typically seen along stress fibers (Fig. 7). Furthermore, myosin-II staining was especially intense along marginal bundles and actin arcs, indicating a high myosin-II content.

Extending lamellipodia at cell edges were largely free of myosin-II with the exception of occasional myosin punctae near the base of lamellipodia (Fig. 7a,b see arrows). After contact between adjacent lamellipodia, myosin-II was conspicuously absent or non-detectable in the actin-filament rich contacting lamellar zone straddled by the marginal bundles from adjacent cells (Fig. 7d,f). Disassembly of marginal bundles and assembly of actin arcs at the contact sites correlated with the loss of staining along the length of the

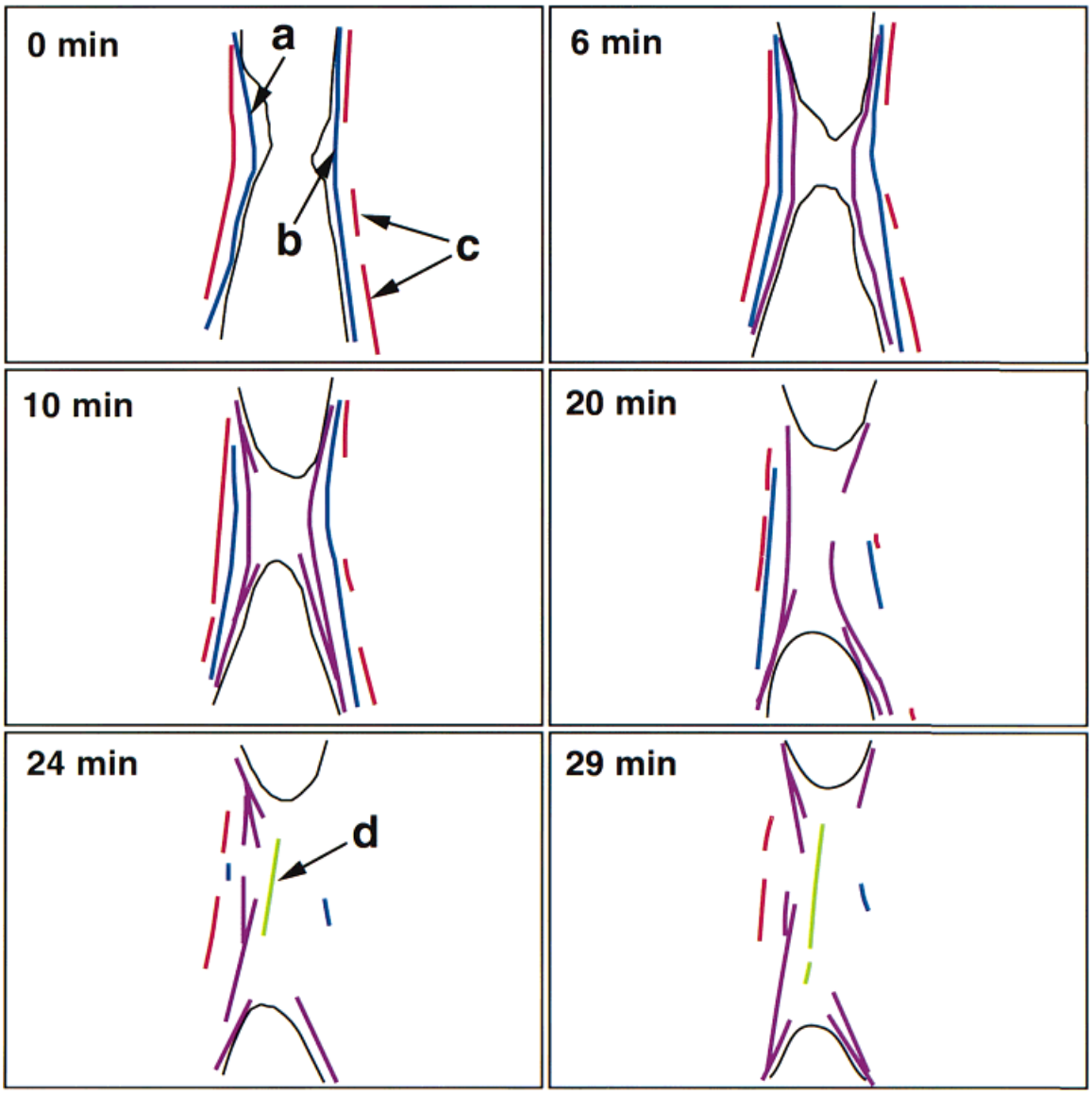

Fig. 5. Schematic representation of actin bundle rearrangements. Color drawings represent positions of actin filament bundles based on the time-lapse observation of rhodamine-phalloidin labeled cells shown in Figure 4. Prior to contact formation (0 min) marginal actin bundles (shown in blue and red) were undergoing rearward flow (compare positions of the blue bundles at 0 and 6 min) and new marginal bundles were formed at the free cell edges (purple). After establishment of an initial contact rearward flow stopped (compare the blue lines at 6 and 10 min). During contact expansion, marginal bundles were rapidly disassembled (see bundle fragments at 20 and 24 min) and new actin bundles were formed along the length of the contact zone (shown in green). Bundles shown in blue correspond to bundles **a** and **b,** red bundles to bundle **c,** and green bundle to bundle **d** in Figure 4.

contact and an increased presence of myosin-II at lateral arcs (Fig. 7f).

DISCUSSION

Use of Low Concentrations of Rhodamine-Phalloidin for Observation of Actin Dynamics in IAR-2 Cells

Because of phalloidin's ability to preferentially bind actin filaments, microinjection of fluorescent phalloidin has been successfully used to analyze the dynamic activity of actin filaments in live cells [Wang, 1987; Wehland and Weber, 1981]. Intracellular concentrations of 2–5 μM phalloidin did not have adverse effects on either actin filament organization or cell motility in fibroblasts and epithelial cells [Wang, 1987; Wehland and Weber, 1981]. For example, cells injected with phalloidin exhibited normal morphology and motility and even successfully completed cytokinesis, an event requiring massive reorganization of the actin cytoskeleton [Wang, 1987]. Consequently, judicious intracellular application

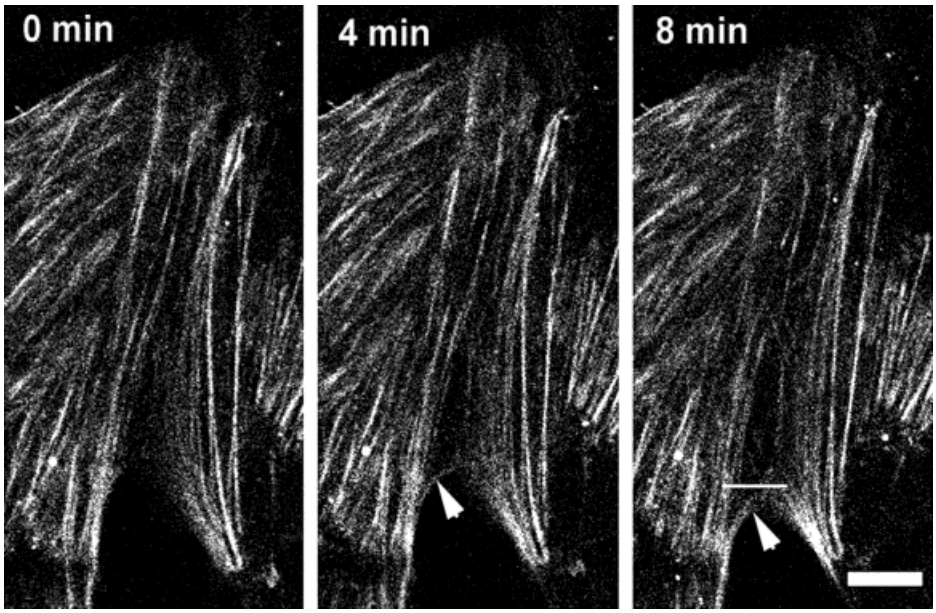

Fig. 6. Contraction of actin arcs during cell-cell contact spreading. An actin filament lateral arc was assembled at the edge of the contact (*arrowhead* at 4 min). The arc then appeared to move with the edge of the cell coincident with lateral expansion of the cell-cell contact. *Arrowhead* at 8 min shows position of the arc and the cell edge after contraction while the white line in the same panel indicates location of the arc prior to contraction. Bar = 10 μm.

of fluorescent phalloidin can be used to provide insight into the structural dynamics of the actin cytoskeleton much the same as loading cells with fluorescent actin analogs.

Brock and co-authors [1996] showed that cell-impermeable molecules were loaded into cells of embryonic epithelium by puncturing the epithelial sheet in the presence of extracellular reagent. It was demonstrated that wounding the epithelium made individual cells transiently permeable to molecules up to 80 kD in size. In the present report, we used the wound loading strategy to efficiently load rhodamine-phalloidin into individual cells lining a scrape-generated wound in monolayers of cultured cells. By having 13 μM rhodamine-phalloidin in the loading solution, we estimated an intracellular phalloidin concentration of ~0.13 μM since, according to Brock et al. [1996], ~1% of the cell volume is loaded during wounding. Consequently, the amount of phalloidin loaded into cells in our experiments is more than an order of magnitude lower than the concentrations used to analyze actin filament dynamics in live fibroblasts [Wang, 1987]. Furthermore, even if 10% of the cell volume was loaded during wounding, the intracellular concentrations of phalloidin would be equivalent to the levels used in prior studies [Wang, 1987].

IAR-2 epithelial cells labeled with rhodamine-phalloidin retained the same organization of the actin cytoskeleton as control, non-labeled cells. Three major classes of actin filament bundles were fluorescently labeled: marginal bundles, stress fibers, and circumferential bundles. Observations of the actin filament meshworks in lamellipodia were not readily possible because of the low concentration of intracellular phalloidin and the limited laser power used to avoid photodamage. Rhodamine-phalloidin labeling of the actin filament meshworks was observed when we increased the loading concentration of phalloidin and used the laser at full power. Previously, Wang [1987] reported that fluorescent phalloidin was not incorporated into actin filaments present within the lamellipodia of fibroblasts. The discrepancy in our observations may be a function of differences in instrumentation sensitivities or in the inherent rates of actin filament turnover in the lamellipodia of fibroblasts vs. epithelial cells. Actin-dependent motility of epithelial cells did not appear to be adversely effected by incorporation of rhodamine phalloidin. Specifically, cells exhibited normal rates of wound closure, forward translocation, and lamellipodial protrusion and retraction. Cells with rhodamine-phalloidin–labeled actin filaments were observed to successfully establish and expand cell-cell contacts at the same rates as control, non-labeled cells. Further, rhodamine-phalloidin–labeled actin filaments retained their sensitivity to depolymerization with cytochalasin B. Based on our observations, it is concluded that rhodamine-phalloidin–loaded IAR-2 cells retain normal physiological function, thus providing a model to examine the role of the actin cytoskeleton in formation and organization of adherens junctions.

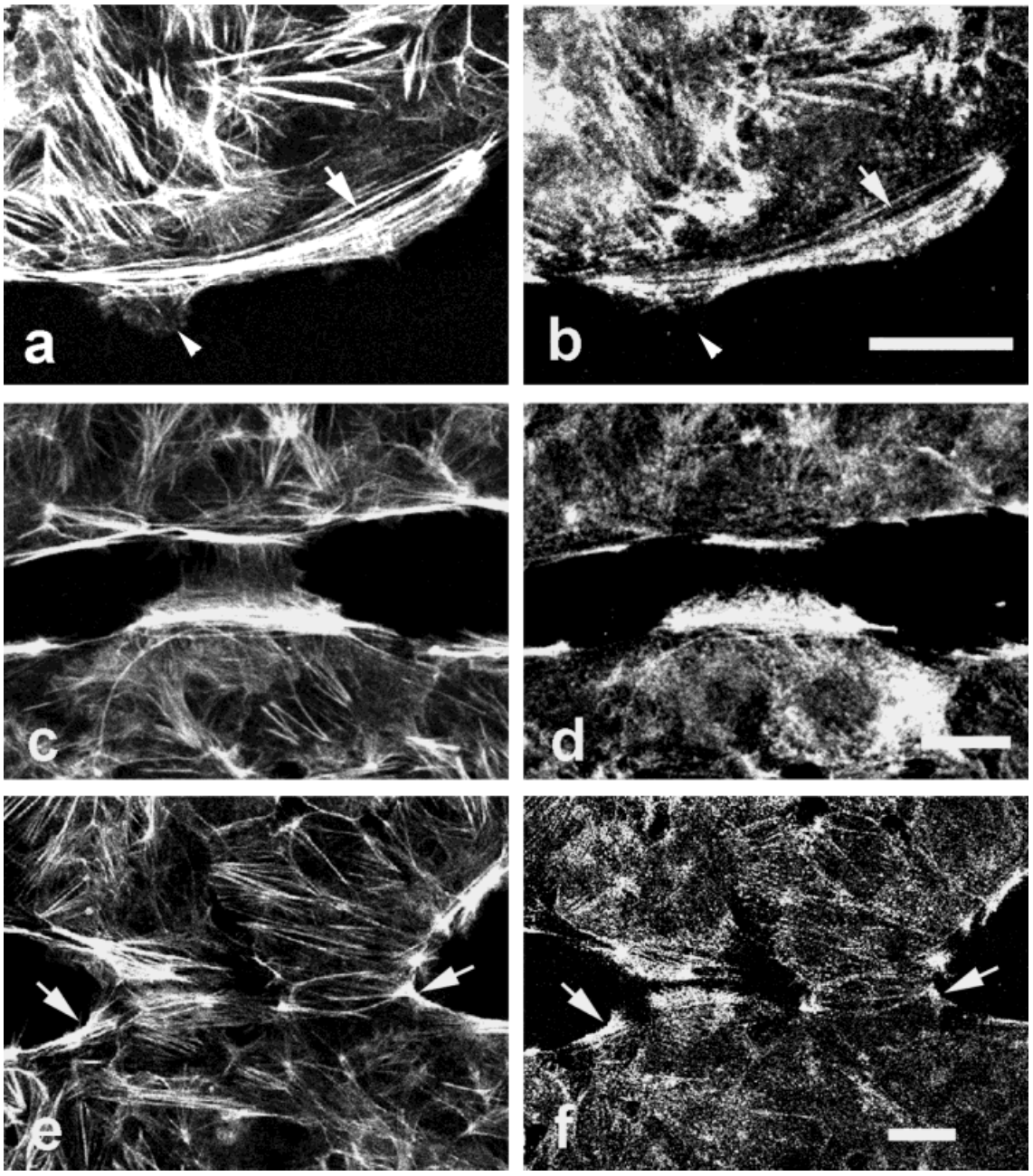

Fig. 7. Localization of actin filaments and myosin-II during cell-cell contact formation. IAR-2 cells were fixed at different stages of contact formation and stained using rhodamine-phalloidin (**a, c, e**) and polyclonal anti-myosin-II antibodies (**b, d, f**). Cells at the free edge of a wound prior to contact formation contained prominent marginal actin bundles enriched in myosin-II (see *arrows* in a and b) while lamellipodia contained very little myosin (see, for example, an extending lamellipodium indicated by *arrowheads* in a and b). Upon formation of an initial contact by lamellipodia, there was no apparent accumulation of myosin-II at the site of the contact (compare c and d). As contact expansion progressed, marginal actin bundles in contacting cells disappeared while myosin-II-rich actin arcs were formed at the edges of the contact (see *arrows* in e and f). Note that circumferential actin bundles are not visible in these confocal images, which were taken through the basal portions of cells. Bar = 10 μm.

Actin Filament Bundle Dynamics at the Free Wound Edge

A characteristic feature of the actin cytoskeleton in IAR-2 epithelial cells is the marginal actin bundle, which is composed of several parallel bundles of actin filaments located in the proximal part of the lamella, behind the lamellipodia. While the presence of actin bundles oriented parallel to the leading edge is not unique to epithelial cells, marginal bundles in this cell type are particularly pronounced and well organized. In our experi-

ments, we observed individual thin marginal bundles of actin filaments assembling along the entire base of the lamellipodia. There was no detectable evidence of polarized assembly either away from or toward the ends of newly forming bundle of actin filaments. Lamellipodia contain dense meshworks of actin filaments that are presumably undergoing continuous centripetal flow [Welch et al., 1997]. Indirect immunofluorescence studies identified the presence of myosin-II in punctae at the base of lamellipodia and in a striated pattern along the marginal actin bundles. Does the lamellipodial contingent of actin filaments and myosin-II serve as the structural ''bricks and mortar'' used to assemble marginal bundles?

Assembly of marginal bundles from lamellipodial meshworks could occur by a myosin-II driven dynamic network mechanism previously proposed for formation of actin bundles in fibroblasts and fish keratocytes [Svitkina et al., 1997; Verkhovsky et al., 1995]. According to the dynamic network model, bipolar myosin-II filaments form a loose network in lamellipodia where they interact with randomly oriented actin filaments. Translocation of myosin heads toward plus ends of actin filaments results in gradual alignment of the actin filaments into parallel bundles. Thus, if actin polymerization and network contraction occurs simultaneously along the entire leading edge of IAR-2 cells, then newly formed marginal bundles should be aligned parallel to the cell edge, should contain myosin-II, and should be under contractile tension. Our observations of bundle assembly, myosin localization, and bundle shortening are consistent with a model whereby marginal bundles of actin filaments are assembled via a dynamic actin-myosin network [Svitkina et al., 1997; Verkhovsky et al., 1995].

In most IAR-2 cells, marginal bundles exhibited rearward or centripetal flow away from the leading edge. Comparing the rates of centripetal flow at different points along the bundle indicated that the central part of the curved bundle moved faster relative to the substrate than the ends of bundle, which were typically stationary. Thus, as centripetal flow proceeded, the bundle lost its curvature, eventually resulting in a shorter, straight bundle. Additionally, bundles undergoing retrograde flow occasionally snap and the remaining segments continue to shorten and thicken, suggesting the segments are under tension from resident myosin-II. Taken together, these results suggest retrograde movement of marginal actin bundles may be the result of bundle contraction-straightening that is driven by the presence of myosin along the bundle. Previously, Giuliano and Taylor [1990] reported retrograde flow of stress fibers in fibroblasts. In fibroblasts, the entire stress fibers move centripetally as a unit whereas in epithelial, the marginal bundles have relatively stationary ends and centripetal flow results from the change in shape of the actin bundle. The centripetal movement we report for marginal bundles appears to be different from that reported for stress fibers in fibroblasts and may represent a previously unrecognized form of centripetal flow. Further, flow of marginal bundles may be a distinct movement separate from bulk cortical flow of actin filaments since Con-A beads attached to the cell surface migrate at rates different from those measured for marginal bundles [see Gloushankova et al., 1995].

After being transported rearward some marginal bundles appeared to exhibit dynamic breakage, which we termed ''snapping.'' Snapping consisted of the establishment of a non-fluorescent gap in the bundle followed by shortening of the remaining fragments toward the ends of the bundles. The initial non-fluorescent gap could be a result of either severing of actin filaments or disruption of actin filament crosslinking within the bundle, which weakens the bundle, causing it to break under tension from myosin located along the bundle. The localized destabilization of the bundle suggests an involvement of actin-binding proteins, possibly, actin-severing and/or actin-bundling proteins. The activity of these proteins can be potentially regulated by Ca^{2+} to provide spatial separation of the processes of bundle assembly at the leading edge and disassembly in the cell body [Janmey, 1994]. Once the integrity of the bundle is compromised, subsequent shortening of bundle fragments is due to myosin-II driven contraction. Shortening could also have occurred by depolymerization of actin filaments whose ends are now exposed or not stabilized by actin binding proteins. While we do not have direct evidence against such a mechanism, filament disassembly is not consistent with the observed thickening and increased fluorescence intensity as the bundles shorten.

Role of the Actin Cytoskeleton in Cell-Cell Contact Formation

Based on morphological and biochemical analyses, several fundamental stages of cell-cell contact formation have been identified. First, a transient cell-cell contact is established between two cells during protrusion/retraction of lamellipodia [Gloushankova et al., 1997; McNeill et al., 1993]. The next step is formation of a small stable cell-cell contact, which is accompanied by inhibition of both protrusion and retraction of the leading edge and cessation of normal rearward flow of surface proteins [Gloushankova et al., 1997]. The final phase in contact formation is lateral expansion of cell-cell contacts and strengthening of cell-cell adhesion [Angres et al., 1996; Gloushankova et al., 1997; McNeill et al., 1993]. During this last stage, surface proteins are transported along the length of the contact, in the direction of the contact spreading, suggesting an active directional positioning of surface receptors [Gloushankova et al., 1997]. Our observations of actin bundle dynamics provide detailed real time information about the functional and structural

modification of the actin cytoskeleton triggered by initiation and maturation of cell-cell contacts, thereby giving insight into the actin-based mechanisms underlying the stages of contact formation.

The present findings support and extend the observations of Smith [1994] who showed that beads attached to the filopodia of cultured neurons could switch their direction of movement from retrograde to anterograde when the filopodia made contact with an adjacent cell. More recently, Suter and colleagues [1998] observed that rearward bulk actin flow in neuronal growth cones is inhibited when immovable substrates became attached to cell surface receptors. During cell-cell contact, cell adhesion molecules present on the surface of the adjacent cell may play the role of such an immovable substrate. Suter et al. [1998] described this activity by the substrate-cytoskeletal coupling model [Lin and Forscher, 1995; Mitchison and Kirschner, 1988] whereby restraining a bead on the cell surface imparts a tensional force that counterbalances the forces driving retrograde flow of actin. When the counter-tension is of sufficient magnitude, there results a loss of cortical actin flow. In the case of cell-cell contact formation, formation of an initial stable contact provides a restraining force to retrograde actin flow leading to local pooling of adhesion molecules that would normally be swept away by the actin current. Once pooled at the cell's edge, the cadherins would then begin construction of stable contacts associated with actin filaments polymerizing at the leading edge of the cell. Whether the coupling of immobile cell surface molecules with inhibition of retrograde flow of both cortical actin and marginal bundles is purely dependent upon mechanical tension or is also reliant upon other cellular activities such as intracellular signaling remains an important question for future investigation.

Cell-cell contact also induced an approximate two-fold increase in the frequency of marginal bundle snapping. Since many bundles were almost completely disassembled over a period of several minutes, this process appears to be a regulated event that is somehow triggered by contact formation. Contact-activated signal transduction is likely to participate in structural reorganization of the cytoskeleton with Ca^{2+} signaling being a prime candidate, given its importance to myosin contractility and regulation of certain actin binding proteins [Janmey, 1994; Tan et al., 1992]. Although data concerning Ca^{2+} transients associated with adherens junctions formation are presently not available, at least one member of the classic cadherin family, N-cadherin, is known to be involved in Ca^{2+}-mediated signaling events [Bixby et al., 1994]. Signal transduction initiating actin reorganization is also likely to involve activity of the Rho family of G-proteins, previously implicated in formation of cell-cell contacts and regulation of the actin cytoskeleton [Braga et al., 1997; Brock et al., 1996; Tapon and Hall, 1997].

Subsequent to cessation of centripetal flow and induced disassembly of bundles, lateral actin arcs formed at the cell-cell boundary. The arcs appeared to move or contract simultaneously with the expansion of the cell-cell contact. Given the localization of myosin-II to the actin arcs, a likely possibility is that myosin-driven contraction may mediate the movement of the arcs and expansion of the contact. Wound closure by expansion of cell-cell contacts may be analogous to previous ''purse-string models'' of actin- and myosin-driven closure of small circular wounds in epithelial monolayers [Bement et al., 1993].

Another major change in actin organization during cell-cell contact formation in epithelial cells is replacement of marginal actin bundles with circumferential actin belts. It is reasonably clear from our observations that marginal bundles were not transformed into circumferential bundles as has previously been proposed [Yonemura et al., 1995]. The data suggest that as expansion of the cell-cell contact proceeds, new bundles of actin filaments form de novo along the cell-cell boundary. Adams and co-authors [1996] have previously observed assembly of spot-like E-cadherin/catenin/actin complexes in newly formed contacts and concluded that contact spreading occurred by gradual addition of such punctae. In some of our experiments, actin bundles at the cell-cell boundary appeared to assemble from small aggregates of fluorescently labeled actin; however, it is unclear whether these actin spots are the cadherin-associated actin punctae observed by Adams and colleagues [1996]. It is most likely that accumulation of cell adhesion molecules and actin filaments in the contact area is followed by assembly of more structured actin bundles, which eventually form adhesion belts along the cell periphery. This gradual maturation of adherens junctions-actin complexes is in agreement with the observations of gradual, actin-dependent strengthening of cell-cell adhesion during establishment of contacts by MDCK cells [Angres et al., 1996]. The bundles formed along the cell-cell boundary would then serve as the precursors of circumferential bundles found in association with mature adherens junctions in epithelial monolayers.

Based on our observations of actin dynamics during contact formation, the following model is proposed for the role of the actin cytoskeleton in contact assembly (Fig. 8). Formation of initial cell-cell contacts occurs primarily as a result of protrusive activity at the leading edge of the cell, which is driven by actin filament polymerization and retrograde cortical flow. Clustering of cell adhesion receptors at the site of the initial cell-cell contact alters local tension gradients, triggering inhibition of retrograde flow of both cortical actin and marginal

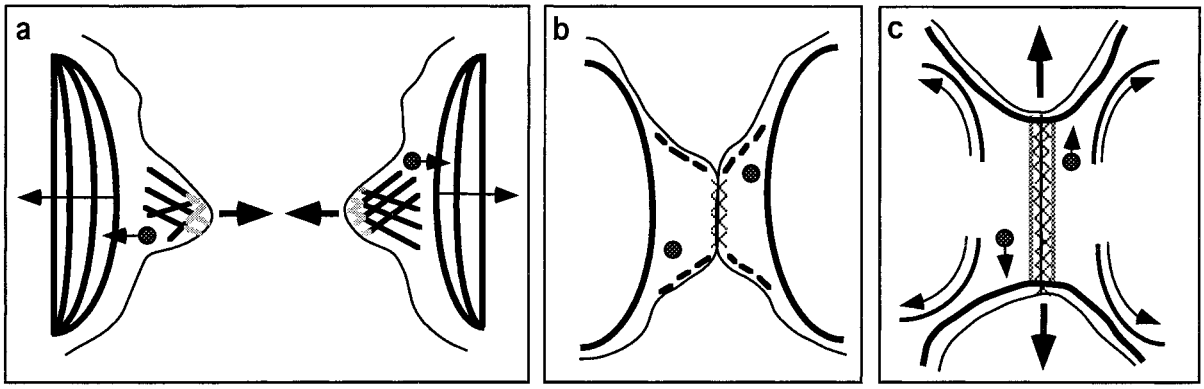

Fig. 8. Actin-dependent mechanism of contact formation in epithelial cells. Prior to contact formation (**a**), the actin cytoskeleton at the leading edge of epithelial cells consists of filament networks in lamellipodia and marginal actin bundles. Marginal actin bundles undergo rearward flow as a result of myosin-dependent contraction-straightening (*thin arrows*). Beads attached to the cell surface (*circles with arrows*) also undergo retrograde transport, however at a rate different from the flow of marginal bundles. Actin polymerization at the leading edge (gray lines) drives lamellipodial protrusion (*large arrows*), which leads to establishment of initial cell-cell contacts (**b**). Clustering of cell adhesion receptors such as E-cadherin at the site of the initial contact (*crosses*) leads to reorientation of tension forces in contacting cells, which results in inhibition of rearward flow. Formation of an initial cell-cell contact also triggers assembly of actin arcs (*dashed lines*) at the edges of the contact. During contact spreading (**c**) tension produced by actin arcs results in lateral expansion of the contact (*big arrows*) and lateral bead translocation. Marginal actin bundles disassemble and contract toward the edges of the contact while new actin bundles assembled at the site of the contact (*stippled lines*) serve to strengthen cell-cell adhesion.

actin bundles. The absence of retrograde flow of actin limits retrieval of surface receptors, thereby promoting further accumulation of cell adhesion molecules in the contact zone. Activated surface receptors elicit signaling events leading to disassembly of marginal actin bundles and formation of actin arcs at the edges of the contact. Myosin-II mediated tension along the lateral arcs of actin results in spreading of the contact while simultaneously aligning newly assembled bundles of actin along the contacting edge. The bundles at the site of contact become associated with adherens junction components, thereby strengthening the contact. Thus, formation of stable intercellular contacts by epithelial cells is dependent upon the coordinated activities of actin filament bundles, myosin-II, and cell adhesion proteins.

ACKNOWLEDGMENTS

We graciously acknowledge the assistance, discussion, and support of our lab colleagues, Volodia Sirotkin and Tim Mure. Very special thanks are extended to Jury Vasiliev and Natasha Gloushankova for their boundless energy, encouragement, and insight into the world of epithelial cells. Additionally, we thank Doug Fishkind for discussions about the use of fluorescent phalloidin to follow actin filament dynamics. This work was partially done during the tenure of a predoctoral fellowship award from the American Heart Association, NJ Affiliate, Inc., to M.K. and is being submitted to the Graduate Faculty of Rutgers University in partial fulfillment of the requirements for the degree of Doctor of Philosophy. This work was supported by a grant from the Charles and Johanna Busch Memorial Fund to E.B.

NOTE ADDED IN PROOF

Avi movies corresponding to Figures 2 and 4 can be viewed at the following website: http://biology-newark.rutgers.edu/cellbio/

REFERENCES

Adams CL, Nelson WJ. 1998. Cytomechanics of cadherin-mediated cell-cell adhesion. Curr Opin Cell Biol 10:572–577.

Adams CL, Nelson WJ, Smith SJ. 1996. Quantitative analysis of cadherin-catenin-actin reorganization during development of cell-cell adhesion. J Cell Biol 135:1899–1911.

Angres B, Barth A, Nelson WJ. 1996. Mechanism for transition from initial to stable cell-cell adhesion: kinetic analysis of E-cadherin-mediated adhesion using a quantitative adhesion assay. J Cell Biol 134:549–557.

Bement WM, Forscher P, Mooseker MS. 1993. A novel cytoskeletal structure involved in purse string wound closure and cell polarity maintenance. J Cell Biol 121:565–578.

Bixby JL, Grunwald GB, Bookman RJ. 1994. Ca2+ influx and neurite growth in response to purified N-cadherin and laminin. J Cell Biol 127:1461–1475.

Braga VM, Machesky LM, Hall A, Hotchin NA. 1997. The small GTPases Rho and Rac are required for the establishment of cadherin-dependent cell-cell contacts. J Cell Biol 137:1421–1431.

Brock J, Midwinter K, Lewis J, Martin P. 1996. Healing of incisional wounds in the embryonic chick wing bud: characterization of the actin purse-string and demonstration of a requirement for Rho activation. J Cell Biol 135:1097–1107.

Cao L-G, Wang Y-L. 1990. Mechanism of the formation of contractile ring in dividing cultured animal cells. I. Recruitment of preexisting actin filaments into the cleavage furrow. J Cell Biol 110:1089–1095.

Cooper JA. 1987. Effects of cytochalasin and phalloidin on actin. J Cell Biol 105:1473–1478.

Geiger B, Yehuda-Levenberg S, Bershadsky AD. 1995. Molecular interactions in the submembrane plaque of cell-cell and cell-matrix adhesions. Acta Anat 154:46–62.

Giuliano KA, Taylor DL. 1990. Formation, transport, contraction, and disassembly of stress fibers in fibroblasts. Cell Motil Cytoskeleton 16:14–21.

Gloushankova NA, Krendel MF, Sirotkin VA, Bonder EM, Feder HH, Vasiliev JM, Gelfand IM. 1995. Dynamics of active lamellae in cultured epithelial cells: effects of expression of exogenous N-ras oncogene. Proc Natl Acad Sci U S A 92:5322–5325.

Gloushankova NA, Alieva NA, Krendel MF, Bonder EM, Feder HH, Vasiliev JM, Gelfand IM. 1997. Cell-cell contact changes the dynamics of lamellar activity in nontransformed epitheliocytes but not in their ras-transformed descendants. Proc Natl Acad Sci U S A 94:879–883.

Gloushankova NA, Krendel MF, Alieva NO, Bonder EM, Feder HH, Vasiliev JM, Gelfand IM. 1998. Dynamics of contacts between lamellae of fibroblasts: essential role of the actin cytoskeleton. Proc Natl Acad Sci U S A 95:4362–4367.

Gumbiner BM. 1996. Cell adhesion: the molecular basis of tissue architecture and morphogenesis. Cell 84:345–357.

Janmey PA. 1994. Phosphoinositides and calcium as regulators of cellular actin assembly and disassembly. Annu Rev Physiol 56:169–191.

Lin CH, Forscher P. 1995. Growth cone advance is inversely proportional to retrograde F-actin flow. Neuron 14:763–771.

McNeill H, Ryan TA, Smith SJ, Nelson WJ. 1993. Spatial and temporal dissection of immediate and early events following cadherin-mediated epithelial cell adhesion. J Cell Biol 120:1217–1226.

Mitchison T, Kirschner M. 1988. Cytoskeletal dynamics and nerve growth. Neuron 1:761–772.

Ozawa M, Ringwald M, Kemler R. 1990. Uvomorulin-catenin complex formation is regulated by a specific domain in the cytoplasmic region of the cell adhesion molecule. Proc Natl Acad Sci U S A 87:4246–4250.

Smith CL. 1994. Cytoskeletal movements and substrate interactions during initiation of neurite outgrowth by sympathetic neurons in vitro. J Neurosci 14:384–398.

Suter DM, Errante LD, Belotserkovsky V, Forscher P. 1998. The Ig superfamily cell adhesion molecule, apCAM, mediates growth cone steering by substrate-cytoskeletal coupling [see comments]. J Cell Biol 141:227–240.

Svitkina TM, Verkhovsky AB, McQuade KM, Borisy GG. 1997. Analysis of the actin-myosin II system in fish epidermal keratocytes: mechanism of cell body translocation. J Cell Biol 139:397–415.

Tan JL, Ravid S, Spudich JA. 1992. Control of nonmuscle myosins by phosphorylation. Annu Rev Biochem. 61:721–759.

Tapon N, Hall A. 1997. Rho, Rac and Cdc42 GTPases regulate the organization of the actin cytoskeleton. Curr Opin Cell Biol 9:86–92.

Verkhovsky AB, Svitkina TM, Borisy GG. 1995. Myosin II filament assemblies in the active lamella of fibroblasts: their morphogenesis and role in the formation of actin filament bundles. J Cell Biol 131:989–1002.

Wang Y-L. 1987. Mobility of filamentous actin in living cytoplasm. J Cell Biol 105:2811–2816.

Wehland J, Weber K. 1981. Actin rearrangement in living cells revealed by microinjection of a fluorescent phalloidin derivative. Eur J Cell Biol 24:176–183.

Welch MD, Mallavarapu A, Rosenblatt J, Mitchison TJ. 1997. Actin dynamics in vivo. Curr Opin Cell Biol 9:54–61.

Yap AS, Brieher WM, Gumbiner BM. 1997. Molecular and functional analysis of cadherin-based adherens junctions. Annu Rev Cell Dev Biol 13:119–146.

Yonemura S, Itoh M, Nagafuchi A, Tsukita S. 1995. Cell-to-cell adherens junction formation and actin filament organization: similarities and differences between non-polarized fibroblasts and polarized epithelial cells. J Cell Sci. 108:127–142.